nature materials

Perspective

https://doi.org/10.1038/s41563-024-01950-9

Engineered moiré photonic and phononic superlattices

Received: 25 August 2022

Accepted: 13 June 2024

Published online: 30 August 2024

Check for updates

Mourad Oudich[1,2], Xianghong Kong[3], Tan Zhang[3], Chengwei Qiu[3] ✉ & Yun Jing[1] ✉

Recent discoveries of Mott insulating and unconventional superconducting states in twisted bilayer graphene with moiré superlattices have not only reshaped the landscape of 'twistronics' but also sparked the rapidly growing fields of moiré photonic and phononic structures. These innovative moiré structures have opened new routes of exploration for classical wave physics, leading to intriguing phenomena and robust control of electromagnetic and mechanical waves. Drawing inspiration from the success of twisted bilayer graphene, this Perspective describes an overarching framework of the emerging moiré photonic and phononic structures that promise novel classical wave devices. We begin with the fundamentals of moiré superlattices, before highlighting recent studies that exploit twist angle and interlayer coupling as new ingredients with which to engineer and tailor the band structures and effective material properties of photonic and phononic structures. Finally, we discuss the future directions and prospects of this emerging area in materials science and wave physics.

Van der Waals heterostructures are two-dimensional (2D) atomic-layer heterostructures in which the interlayer binding is achieved through weak van der Waals interactions[1]. The study of how the relative twist angle between successive layers in van der Waals heterostructures can be used to manipulate the material's electronic properties is often referred to as twistronics[2]. An increasingly important topic in twistronics is twisted bilayer graphene (TBG), where two graphene sheets are arranged one on top of the other with a slight angle of misalignment[3]. Such a small twist results in a moiré superlattice at a much larger length scale than the underlying graphene lattice, radically changing the band structure of bilayer graphene with the more conventional AA-stacked or AB-stacked (Bernal) configurations, which in turn gives rise to unconventional electronic[4,5], optical[6,7] and thermal properties[8] of TBG. One of the most extraordinary features of TBG is the emergence of zero-energy-level flat bands at a series of so-called magic angles.

In 2011, Bistritzer and MacDonald reported that the Dirac-point velocity vanishes at some magic angles (the smallest being around 1.05°)[5], and that nearly flat bands emerge at the magic angle, which contributes a sharp peak to the Dirac-point density of states (DOS). This study marked an important milestone for theoretical work in twistronics. It was not until 2018 that magic-angle bilayer graphene was experimentally confirmed by the group of Jarillo-Herrero at Massachusetts Institute of Technology[9,10]. Their back-to-back papers in *Nature* reported two important discoveries pertaining to magic-angle bilayer graphene: correlated (or Mott) insulation[9] and unconventional superconductivity at around 1.7 K (ref. 10). These two discoveries have generated a host of theoretical and experimental papers seeking to better understand and further explore the different phenomena associated with magic-angle TBG[11–13].

Taking inspiration from TBG, researchers in classical waves have attempted to use the twist degree of freedom as a new dimension for expanding the design space of synthetic photonic and phononic structures, such as photonic crystals and phononic crystals. For example, stacking two photonic crystals or phononic crystals in a honeycomb lattice with a small twist angle (θ) between the two layers constitutes a simple analogue of TBG[14–19]. Using these bilayer twisted photonic and photonic structures, magic angles have been investigated for electromagnetic and mechanical waves, showing a new route for flat band

[1]Graduate Program in Acoustics, Penn State University, University Park, PA, USA. [2]Institut Jean Lamour, CNRS, Université de Lorraine, Nancy, France. [3]Department of Electrical and Computer Engineering, National University of Singapore, Singapore, Singapore. ✉e-mail: chengwei.qiu@nus.edu.sg; yqj5201@psu.edu

https://doi.org/10.1038/s41563-024-01950-9

BOX 1

The moiré pattern

The moiré pattern is a well-known visual effect that can be observed when at least two planar periodic structures, such as grids or gratings, are superposed or overlaid close to each other with a misalignment such as an angular twist. The moiré pattern is often seen as an alternation of dark and bright areas, where the bright areas are created when the two layers largely overlap, while the dark areas are ones where the two layers overlap to a much lesser extent. The moiré pattern is highly sensitive to geometrical displacement and rotation of one layer with respect to the other, which renders the moiré-inspired system an extremely dynamic platform for a wide range of applications such as the measurement of displacement[77] and movement[78]. Moiré patterns have also been used historically for marine navigation in shoreside beacons known as 'Inogon lights' to indicate safe paths for ships and prevent them from running into underwater cables and pipelines.

In condensed matter physics, moiré patterns are typically created from angular misalignment between a pair of atomic monolayers. Of particular interest is TBG, largely due to the zero-energy-level flat bands at the magic angles. Here, we delineate the geometrical construction of the moiré superlattice from the twisting two monolayers of atoms. Let the periodicity of the first lattice be governed by two primitive lattice vectors $\mathbf{a}_1$ and $\mathbf{a}_2$. The position of each unit cell (atom) can be then described by the vector $\mathbf{R}_a=n_1\mathbf{a}_1+n_2\mathbf{a}_2$, where n_1 and n_2 are integers. Assuming that the second lattice is identical to the first one but rotated by an angle θ, each unit cell in the second lattice will be located at $\mathbf{R}_{a'}=m_1\mathbf{a}'_1+m_2\mathbf{a}'_2$, where m_1 and m_2 are integers and $\mathbf{a}'_1$ and $\mathbf{a}'_2$ are vectors after rotation of $\mathbf{a}_1$ and $\mathbf{a}_2$. In the (x, y) plane, if we adopt the complex notation $a_k=a_{k,x}+ja_{k,y}$, where $a_{k,x}$ and $a_{k,y}$ are the coordinates of the vector $\mathbf{a}_k$ (k=1, 2), where the complex number $j^2=-1$, then one can write $a'_k=a_k e^{j\theta}$, which leads to $R_{a'}=m_1a'_1+m_2a'_2=(m_1a_1+m_2a_2)e^{j\theta}$. In general, the equality $R_{a'}=R_a$ is not necessarily valid for any set of integers n_1, n_2, m_1 and m_2, meaning that the resulting moiré patterns are not guaranteed to be perfectly periodic—they can be instead quasiperiodic. These twist-induced moiré patterns, however, can become perfectly periodic for discrete values of θ, which can be determined by the set of n_1, n_2, m_1 and m_2 that lead to $R_{a'}=R_a$. These angles, known as commensurate angles, can be given by equation (1), as long as the solution is a real number[59]:

$$\theta = j\ln\left(\frac{n_1a_{1,x}+n_2a_{2,x}+j(n_1a_{1,y}+n_2a_{2,y})}{m_1a_{1,x}+m_2a_{2,x}+j(m_1a_{1,y}+m_2a_{2,y})}\right). \quad (1)$$

A trivial solution would be $m_1=n_1$ and $m_2=n_2$, which corresponds to θ=0.

For the case of triangular, honeycomb and kagome lattices, the periodicity can be defined by the set of vectors $\mathbf{a}_1=a(1, 0)$ and $\mathbf{a}_2=a\left(1/2, \sqrt{3}/2\right)$, where a is equal to p, $\sqrt{3}p$ or $2p$ for the triangular, honeycomb or kagome lattice, respectively, and p is the distance between closest atoms. Subsequently, equation (1) becomes

$$\theta = j\ln\left(\frac{2n_1+n_2+jn_2\sqrt{3}}{2m_1+m_2+jm_2\sqrt{3}}\right). \quad (2)$$

However, in the case of twisted bilayer square lattices, equation (1) becomes,

$$\theta = j\ln\left(\frac{n_1+jn_2}{m_1+jm_2}\right). \quad (3)$$

Then, θ being real valued requires $m_1^2+m_2^2+m_1m_2=n_1^2+n_2^2+n_1n_2$ for triangular, honeycomb and kagome lattices, whereas this relation becomes $m_1^2+m_2^2=n_1^2+n_2^2$ for the case of the square lattice. Apart from the trivial solution, one can consider the solution $m_1=n_2$ and $m_2=n_1$ that gives the commensurate angles of the twisted bilayer lattices. Panel **a** shows the discrete commensurate angles as a function of these integers for twisted bilayers with triangular, honeycomb and kagome lattices (top) and the square lattice (bottom).

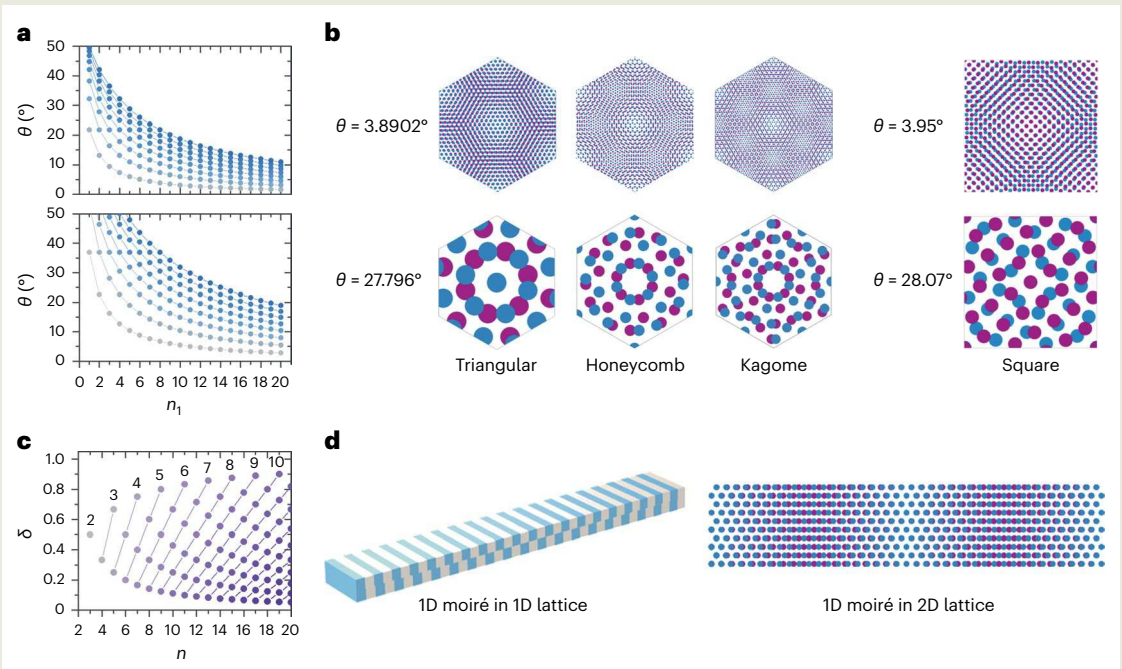

(continued from previous page)

Each line of connected dots corresponds to a value of n_2 that varies from n_1+1 (grey) to n_1+8 (blue). These plots suggest that the distribution of commensurate angles in the case of triangular, hexagonal or kagome lattices is slightly denser in comparison with that of the twisted bilayer square lattice. In addition, panel **b** shows examples of unit cells of the moiré superlattices for one small (top row) and one large (bottom row) commensurate twist angle. The number of atoms per unit cell is greater for the twisted bilayer kagome lattice than for the honeycomb and triangular lattices. Note that the superlattices are drawn in a way that they have the identical size for different cases, resulting in the atoms appearing to have varying sizes.

Among these four types of twisted bilayer lattice, the most frequently studied one is TBG (honeycomb lattice) with the exploration of its electronic[5,9–12,79], optical[6,7,80–82] and thermal properties[8,83,84]. Meanwhile, fewer studies have explored the electronic dispersion of twisted bilayer triangular lattices using WSe_2 (ref. 85), $MoSe_2/WSe_2$ (ref. 86), WSe_2/WS_2 (ref. 87) and transition metal dichalcogenides[88], whereas other studies have investigated twisted bilayer kagome lattices[89,90] and square lattices[43,45,91,92].

Moiré patterns can also be created by considering two lattices with a mismatch in their periodicities along a specific direction. Consider a 1D periodic lattice with a period of a and a second lattice with a period of $a'=a+\delta a$, where $0<\delta<1$; then, stacking the two lattices will yield a 1D moiré pattern. This pattern is generally quasiperiodic but can also be perfectly periodic for discrete values of δ, which can be found using the equation $na=ma'$, where n and m are integers. This leads to the relation $\delta=(n-m)/m$ with the condition of $1<n/m<2$. Panel **c** shows the values of δ as a function of n and m (the number indicated for each line of connected dots is the value of the integer m), whereas panel **d** presents examples of a 1D moiré superlattice created from two 1D lattices (left) and a 1D moiré superlattice created from two layers of triangular lattices with a periodicity mismatch in the horizontal direction (right). These bilayer 1D moiré patterns in classical waves have been studied less extensively than 2D moiré patterns, and the relevant studies have been focused mainly on optics[50,51]. Finally, the mismatch in periodicity can also be created in both spatial directions[93].

engineering in synthetic moiré photonic and phononic structures. Some of the moiré photonic and phononic bilayer designs go beyond merely mimicking magic-angle bilayer graphene. One example in this regard is the demonstration of polariton topological transition in bilayers of α-phase molybdenum trioxide (α-MoO_3)[20], where the polariton dispersion can be precisely controlled by the twist angle and shows a transition point at a fundamentally different magic angle from the one in TBG. This work exemplifies how researchers can draw inspiration from TBG to introduce new design models for enabling optical and acoustic properties that are unavailable in monolayer synthetic photonic and phononic structures.

In this Perspective, we showcase recent developments in the field of moiré classical wave structures. Specifically, we introduce the moiré pattern and its underlying mathematics (Box 1). We provide a general guideline for the design of photonic and phononic moiré structures (Box 2), followed by a detailed examination of these two types of structure. Our discussion examines the construction of moiré superlattices, the characterization of their wave dispersion behaviour, and the customization of their twist angle and interlayer coupling strength to realize unique wave phenomena for both electromagnetic and mechanical waves. Moreover, we also address the challenges and routes for applications in this field, and conclude by highlighting the future directions for the development of photonic and phononic moiré structures. We would highlight that there is a recent review paper on moiré photonics and optoelectronics[21]. Our paper, in turn, offers a complementary perspective to further illuminate the emerging field of moiré physics.

Moiré photonic structures

The generalized concept of homogeneous crystals is considered valid when the behaviour of a crystal can be modelled using effective medium theory. For photonics (or phononics), such a concept goes hand in hand with the long wavelength approximation, under which the crystal can be greatly simplified by taking its average electromagnetic (or mechanical) response—a process known as homogenization. For instance, certain natural crystals (for example, black phosphorus[22], α-MoO_3 (refs. 20,23,24) and WTe_2 (ref. 25)) and nanostructured crystals with deep subwavelength periodicity (for example, graphene and hexagonal boron nitride nanoribbon arrays[26,27]) can be treated as homogeneous crystals, where an anisotropic surface conductivity tensor can be used to characterize these low-dimensional materials for manipulating light[7]. Owing to dispersion, the imaginary part of the surface conductivity tensor can have opposite signs in the two orthogonal directions within a certain frequency range, where the crystal will behave like a strongly anisotropic 2D material known as a hyperbolic metasurface. When two such hyperbolic metasurfaces are stacked, a moiré metasurface is created (Fig. 1a). The isofrequency contour of the moiré metasurface lies somewhere between those of the two individual metasurfaces due to the coupling effect (Fig. 1b). The isofrequency contour can be analytically derived by first choosing plane waves as the basis for the three domains created by the two metasurfaces (that is, the domain above the top metasurface, the domain in between and the domain below the bottom metasurface) and then matching the boundary conditions of the two metasurfaces that are determined by the surface conductivity tensor. By tuning the twist angle between the two hyperbolic metasurfaces, the isofrequency contour evolves from being hyperbolic to elliptical, which is analogous to the Lifshitz transition in electronics[20,28,29]. The isofrequency contour flattens at a photonic magic angle where the transition from a hyperbolic to an elliptical contour occurs. The self-collimation phenomenon can be detected at the magic angle as the group velocity direction is fixed due to the flattened isofrequency contour (Fig. 1c)[20,30].

In addition to the electrical surface conductivity, chiral surface conductivity was also discovered in photonic TBG metasurfaces when retrieving the effective electromagnetic parameters[31–34]. The opposite chirality can be created simply via the relative rotation of the two layers which have mirror symmetry. Note that although graphene can also be considered an optical metasurface, the optical properties of TBG are beyond the scope of this Perspective and the reader is referred to a review paper for a more in-depth discussion on this topic[35].

When the working wavelength is comparable with the unit cell of the crystal, homogenization is no longer valid, and Bloch's theorem can be applied to analyse the photonic crystal's electromagnetic response. The periodicity of the moiré pattern at a commensurate angle is usually much larger than the size of the unit cell of the monolayer. However, in the case of a honeycomb lattice, when the twist angle is 0° (AA stacking) or 60° (AB stacking), the periodicity of the moiré pattern reaches its minimum, which is the same as that of the monolayer (Fig. 1d)[16]. In addition, narrow solitons appear between AB and BA domains, and high local optical conductivity can be observed at the AA domains via

https://doi.org/10.1038/s41563-024-01950-9

BOX 2

Moiré lattices in classical waves

The design of moiré photonic/phononic structures requires multidisciplinary knowledge in materials science, optics, acoustics and engineering. The choice of materials, the periodicity of the moiré pattern, the coupling between the two layers, the band structures of the moiré structure and tunability using external stimuli are important aspects to be considered. In addition, although the differences between photonic and phononic structures in terms of the wave types and the frequency ranges determine the choice of the constituent materials in their design, the general guidelines for designing the moiré photonic and phononic structures are similar. A moiré photonic (phononic) structure is generally created by stacking two layers of photonic (phononic) lattices in a way that facilitates the interaction between the waves supported by each layer. In this case of mimicking TBG, where the interlayer hopping is crucial, the stacking of two photonic (phononic) layers is designed to ensure the interaction between the propagating electromagnetic (mechanical) waves between the two layers. This interaction is usually enabled either by coupling the evanescent wave fields[14,16,19,94] or by introducing a coupling medium between the two layers[18,55]. The strength of the interlayer coupling can be controlled by adjusting the separation distance or the thickness and property of the coupling medium between the layers. The photonic (phononic) dispersion of the moiré structure can be further tailored by the twist of one layer with respect to the other. This design strategy has enabled the observation of band dispersion of classical waves, analogous to the electronic dispersion in TBG for different stacking configurations such as AA and AB[14,16–18,55,60]. Moreover, it has shown the emergence of flat bands for electromagnetic[16–19,94] and mechanical waves[14,15,17] at specific angles. Beyond mimicking the electronic band dispersion of TBG, other photonic (phononic) moiré designs have been developed to enable intriguing phenomena for classical waves. Those moiré platforms were constructed either by stacking periodic lattices[20,26,40,45,50], not necessarily graphene-like, or by moiré patterning the effective properties of the photonic/phononic structure[46,61,95]. In many of these studies, it is not necessarily the interlayer coupling that dictates the wave behaviour. For example, a single layer of moiré pattern has been shown to also support topological transitions in the isofrequency contours for mechanical waves[61]. The choice of the constituent material for the moiré photonic/phononic structure also holds substantial importance, except in the case of acoustic structure. Particularly for airborne sound, the constituent material's role in the acoustic crystal/metamaterial is relatively of little importance. This is because most materials can be treated as acoustically hard compared with air, and therefore their sole purpose is to provide rigid surfaces for channelling the sound.

nano-imaging experiments[6,36]. By creating effective potential wells centred around the AA-stacked region, the intrinsic localized states are obtained, leading to the superflat bands in a wide and continuous parameter space[37]. Hence, a detailed investigation of AA and AB stacking is crucial for understanding the underlying physics of moiré patterns[16]. Figure 1d shows an example in which a photonic crystal layer comprising a metallic plate that features a hexagonal lattice of metallic pillars facilitates the propagation of spoof surface plasmons (SSPs)[38]. The band structure of the SSP that results from such a lattice mimics that of the graphene, with a Dirac cone appearing at the K point of the reciprocal lattice[39]. The stacking of two of these photonic crystal lattices at an appropriate separation distance enables the SSPs from the two layers to interact, leading to a dispersion behaviour that is strikingly similar to that of bilayer graphene[16]. Furthermore, the tight binding model developed in bilayer graphene can be readily used to describe the dispersion of the bilayer photonic crystal in the vicinity of the Dirac frequency with properly fitted parameters[16] (Fig. 1d).

In addition, different quantitative analyses have been applied to the photonic analogy of TBG[19,40]. A silicon disk was used as the photonic counterpart of the carbon atom in graphene (Fig. 1e left)[19]. Coupled mode theory was applied to describe the coupling between nearest-neighbour disks. For simplicity, a continuum model of the interlayer coupling strength was considered to replace the discrete coupling between two disks. Compared with the continuum model for the homogeneous crystals[29] mentioned above, the interlayer coupling strength in coupled mode theory is periodic and has the same periodicity as the moiré pattern. The band diagram and DOS calculated using the continuum model show local flat bands at the photonic magic angles (Fig. 1e right). Similar photonic properties of twisted bilayer photonic honeycomb lattices have also been demonstrated[18], where the band structure was engineered by adjusting the device geometry and a larger band asymmetry was shown in the photonic system. While these two studies[18,19] numerically demonstrated the magic angles in twisted bilayer photonic graphene at the optical frequency, magic angles and topological corner modes were also demonstrated in twisted bilayer photonic graphene at the microwave frequency[16]. Furthermore, these studies[16,18,19] explored the interlayer coupling strength as a degree of freedom to tune the magic angle. Besides the magic-angle flat band hosted by moiré structures, other unusual optical states can also be reached by tuning the angle between two photonic graphene layers. Very recently, evidence for quasi-bound states in the continuum was shown theoretically in a moiré photonic crystal at the terahertz frequency[41]. In addition to the honeycomb lattice, the photonic dispersion of the twisted bilayer square lattice photonic slab was investigated through a high-dimensional plane wave expansion method[40,42] (Fig. 1f). Instead of choosing plane waves as the basis, as mentioned earlier in effective medium theory, Bloch waves were first chosen as the basis of the two slabs and plane waves were used as the basis of the surrounding space. Bloch waves in the slabs were then decomposed into plane waves, and the boundary conditions with the plane waves in the surrounding spaces were matched to collectively give rise to the analytical solution. Strongly tunable resonance properties and chiral behaviour were discovered by observing the transmission under incident light with different frequencies and twist angles. The same types of twisted bilayer photonic crystal slab were also demonstrated to be a tunable narrow stop-band frequency filter[43]. Topological flat bands can be sustained in moiré photonic structures, where topological edge modes deform into higher-order topological corner modes after breaking the reflection symmetry of the boundary of the superlattice[44].

When the twist angle is incommensurate, the photonic moiré pattern becomes aperiodic without translational periodicity although the rotational symmetry still persists[45–47]. Instead of using a bilayer system to generate the moiré pattern, the moiré patterns were projected on to a single surface using optical induction and the weight of the 'two layers' can be tuned during the projection process to generate different moiré patterns[45]. The localization–delocalization transition of light by altering the patterns from incommensurable to commensurable was experimentally demonstrated. As a particular case of the incommensurate lattice, the quasilattice refers to the case when the lattice vectors have an equiangular offset between them and are of equal magnitude[46]. The 45° twist angle in a square lattice or 30° twist angle in a hexagonal lattice can form a quasilattice, which has eight-fold and 12-fold rotational symmetry, respectively (Fig. 1h). Quasilattice patterns with rotational symmetries as high as 36-fold were developed via moiré nanolithography on silver plasmonic crystals[47], and an increased

https://doi.org/10.1038/s41563-024-01950-9

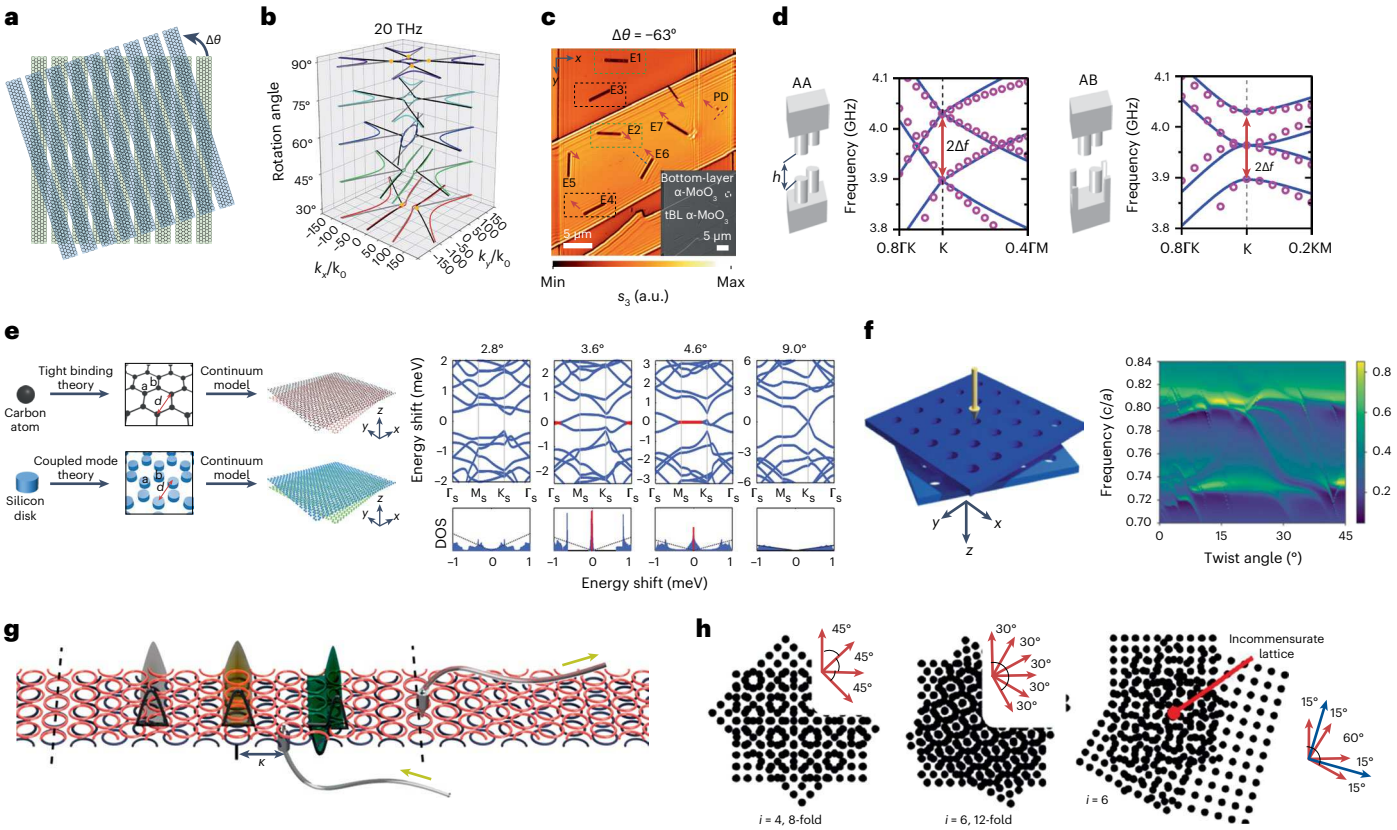

Fig. 1 | Examples of moiré photonic structures. a, The moiré hyperbolic metasurface composed of two coupled uniaxial metasurfaces with a certain twist angle[26]. **b**, Dispersion relations as a function of the twist angle. The grey (black) solid lines denote the dispersion of the first (second) individual metasurface whereas the coloured lines denote the dispersion of the moiré metasurface[26]. k_x and k_y are the x and y components of the wavevector and k_0 is its norm. **c**, Near-field images of the fixed group velocity direction (red arrows) near the magic angle[20]. s_3 is the experimentally measured near-field distribution. Fabricated seven edges 'E' and one point defect 'PD': E1 and E2 are parallel along the [100] crystal axis of the bottom layer, E3 and E4 are parallel along the [001] crystal axis of the top layer, E5 is along the [001] crystal axis of the bottom layer, and E6 and E7 along other directions. Inset: a scanning electron microscopy image of the sample tBL, twisted bilayer. **d**, AA-stacked (left) and AB-stacked (right) bilayer photonic crystals and their associated band structures[16]. h, air-gap thickness; f, frequency. **e**, Left: twisted bilayer photonic structure based on a honeycomb lattice of silicon nanodisks (disk a and disk b) and its comparison with TBG. d is the lattice constant. Right: dispersion curves and DOS with different twist angles showing the existence of local flat bands at certain angles[19]. **f**, Twisted bilayer photonic crystal with circular holes in a square lattice (left) and the transmission (denoted by the colour scale) as a function of the frequency and twist angle (right)[40]. c/a is the frequency unit, where c is the speed of light and a is the lattice constant. **g**, Moiré pattern formed using metallic rings with different periods in the top (red) and bottom (black) layers[50]. κ, deviation of the excitation dipole from the moiré pattern centre. **h**, Eight-fold quasilattice (left), 12-fold quasilattice (middle) and a general incommensurate lattice formed by the overlap of square lattices from two layers (right)[46]. i is the number of exposures for a quasilattice. Panels reproduced with permission from: **a**,**b**, ref. 26, American Chemical Society; **c**, ref. 20, Springer Nature Ltd; **d**, ref. 16, APS; **e**, ref. 19, APS; **f**, ref. 40, APS. Panels adapted with permission from: **g**, ref. 50, APS; **h**, ref. 46, American Chemical Society.

number of surface plasmon polariton modes have been discovered in quasilattices[47]. In a recent study, a theoretical approach based on combining supercell calculation and band unfolding techniques was constructed to globally characterize the photonic dispersion of a 2D quasiperiodic moiré superlattice[48]. Compared with typical near-field moiré photonic crystals, most recently, far-field coupling between moiré photonic architectures has been experimentally observed, where twist-angle-controlled directional lasing emissions were achieved[49].

In addition to the twist between two monolayer crystals, moiré patterns due to mismatched lattice constants have been studied[50–52]. For instance, two parallel hexagonal lattice metallic ring metasurfaces with a lattice constant mismatch in one direction were introduced to form a moiré bilayer system (Fig. 1g)[50]. As the periodicity of the moiré pattern is much larger than the unit cell, the supercell was decomposed into unit cells with different shifts between the two layers, and the relative shift in the unit cell was treated as an effective gauge field created by an artificial magnetic field. The corresponding photonic Landau levels were observed experimentally. Similar results have also been found when overlapping two one-dimensional (1D) photonic crystal slabs with mismatched periods[51–53], where the authors showed a high concentration of the Wannier function in a moiré cell. In a recent study, a 1D moiré silicon photonic nanowire was designed and fabricated to demonstrate a host of behaviours that include slow-light, high-Q-factor moiré resonators, multi-resonant filters, suppression of grating side-bands, persistent versus extinguishable transmission, tunable Q factors and tunable group velocities[54].

Moiré phononic structures

TBG not only sparked substantial interest in developing moiré photonic structures but also spawned the new field of moiré phononic structures for controlling acoustic[14,17,55–58] and elastic waves[15,59–62]. A bilayer sonic structure was proposed, composed of two stacked phononic crystals, where each monolayer phononic crystal is made of a triangular lattice of rigid triangular units[56] (Fig. 2a, left). A perforated rigid plate separates the two phononic crystals, where the holes induce the interlayer coupling. The stacking was of the AA configuration, and the triangular units within each cell were rotated in both layers to give rise to different dispersion behaviours in the vicinity of the Dirac point (Fig. 2a,

https://doi.org/10.1038/s41563-024-01950-9

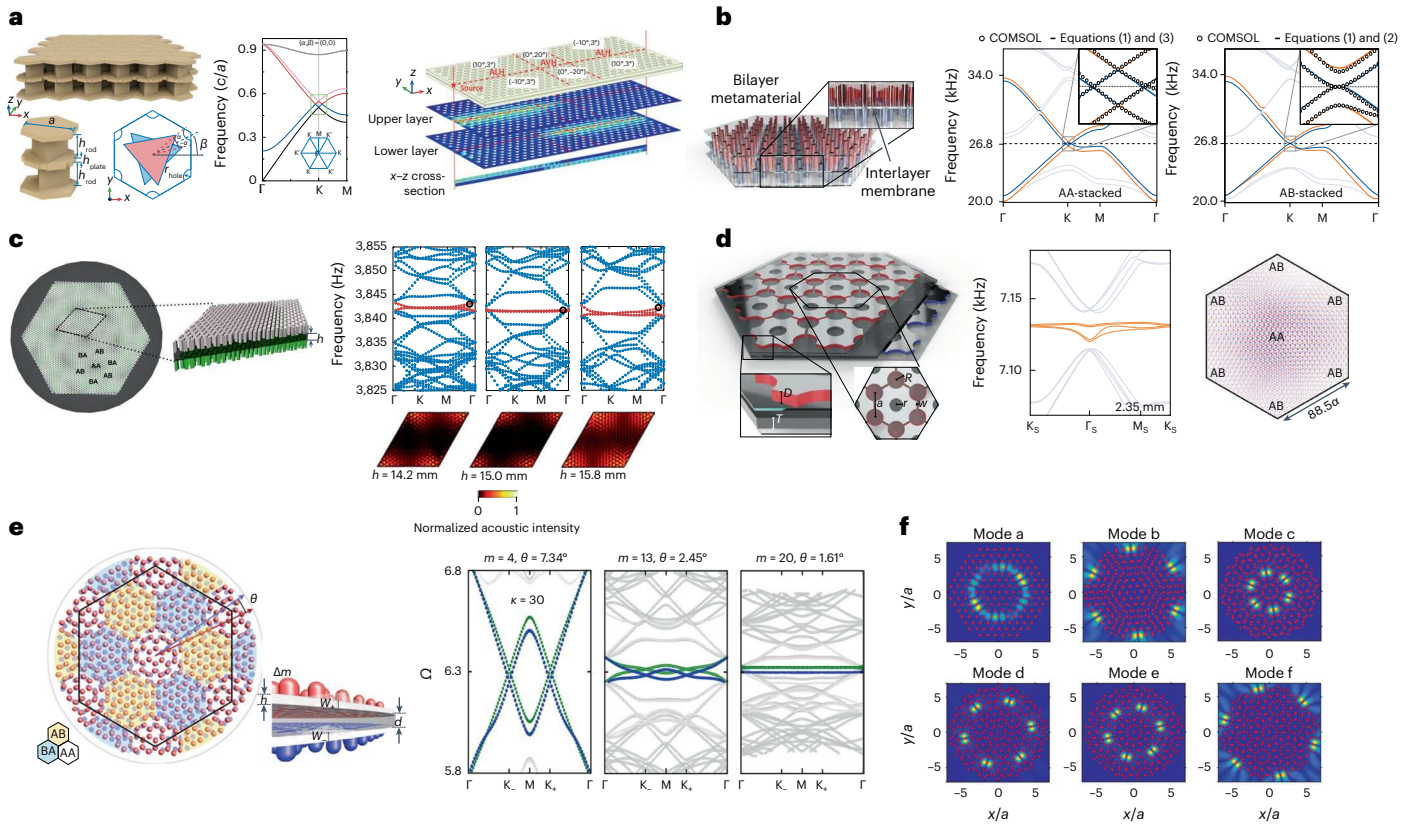

Fig. 2 | Examples of moiré phononic structures. a, Left: bilayer sonic crystal made of two phononic crystals with triangular lattices, and a rigid plate with holes separates the two phononic crystals to enable mode coupling[56]. ALH, acoustic layer-valley Hall; AVH, acoustic valley Hall; α and β, orientation angles of the triangular rods; a, lattice constant; h_{rod}, thickness of the triangular rods; h_{plate}, thickness of the plate; r_{hole}, radius of the holes. Middle: band dispersion that shows crossing bands for AA stacking. Right: bilayer valley Hall transport from the upper layer to the lower layer. The colour scale represents the acoustic pressure amplitude. **b**, Left: bilayer metamaterial made of two acoustic lattices of rigid cylinders in air separated by a thin vibrating membrane to mimic the interlayer hoping[55]. Right: band dispersions for AA and AB stacking. **c**, Left: twisted bilayer sonic crystal consisting of two rigid plates with air cavities facing each other, where each plate supports the propagation of SSAWs[14]. Right: band structures at a fixed twist angle of 3.481° for different interlayer couplings via changing the air-gap thickness between the rigid plates. The acoustic intensity in the moiré supercell is plotted near the Γ point, for the bands marked in red. **d**, Left: acoustic bilayer structure created from stacking two sonic crystals, each made of connected cavities. The sonic crystals are separated by a vibrating membrane[17]. D, steel layer thickness; T, membrane thickness; a, cavity spacing; r, central cavity radius; w, channel width; R, is the cavity radius. Right: flat bands created at the magic angle with confined acoustic energy at the AA regions of the moiré supercell. **e**, Twisted elastic bilayer lattice made of two coupled plates decorated with honeycomb lattices of pillars (left), giving rise to flat bands at the magic angle (right)[15]. h, thickness of the plate; Δm, mass; W_+ and W_-, the flexural waves amplitude the for upper and lower layers, respectively; d, thickness of the coupling medium; Ω, normalized frequency; κ, coupling parameter. **f**, Moiré lattices made of a cluster of scatterers showing dipolar resonances at discrete values of the twist angle[59]. The colour scale represents the acoustic field pattern. Panels reproduced with permission from: **a**, ref. 56, APS; **b**, ref. 55, APS; **c**, ref. 14, APS; **d**, ref. 17, IOP; **e**, ref. 15, APS. Panel **f** adapted with permission from ref. 59, APS.

middle). The existence of two types of topological valley edge state was numerically and experimentally demonstrated, with interfaces that support either valley Hall states propagating in both layers or layer-valley Hall states that mainly propagate in a single layer. Topological waveguiding with propagation from one layer to the other was also experimentally demonstrated (Fig. 2a, right). Although this work does not directly involve moiré patterns, it is one of the earliest studies that provide crucial insight into how interlayer coupling and rotation can be harnessed to engineer the dispersion of bilayer phononic crystals. A bilayer phononic crystal consisting of rigid cylindrical rods in a honeycomb lattice was designed where the two layers were separated by a thin vibrating membrane to ensure the interlayer coupling of acoustic waves[55] (Fig. 2b, left). By choosing the appropriate interlayer coupling strength via changing the thickness and density of the membrane, the authors numerically showed that the acoustic dispersion of the bilayer can mimic the electronic dispersion of the classical bilayer graphene near the Dirac cone frequency for both AA and AB stacking configurations with two sets of crossing Dirac bands and quadratic dispersion, respectively (Fig. 2b, right). Shortly afterwards, the twist degree of freedom was considered in a sonic bilayer crystal where each layer is a rigid plate with a honeycomb lattice of cylindrical air cavities[14] (Fig. 2c, left). Each phononic crystal plate supports spoof surface acoustic waves (SSAWs) propagating in the near field above the air cavities with evanescent decay in the direction perpendicular to the plate surface. By positioning the phononic plates to face each other with an air gap in between, the SSAWs supported by each plate can interact, mirroring the interlayer hopping in bilayer graphene. Moreover, twisting one plate with respect to the other creates a moiré pattern, and it was numerically shown that at specific twist angles (magic angles), flat bands appear with confined acoustic intensity in the AA regions of the moiré superlattice (Fig. 2c, right).

The magic angle depends strongly on the interlayer coupling strength and can be tuned by varying the distance between the phononic crystals. A bilayer twisted acoustic metamaterial was designed using a vibrating polyethylene membrane as the coupling medium[17] (Fig. 2d, left). The authors also numerically showed the trapping of sound via the twist that is associated with the flattening of the Dirac bands at a magic angle of 1.12° (Fig. 2d, right). This magic angle can be

tuned to higher values by changing the interlayer coupling strength through varying the thickness of the membrane. The dispersion of these phononic bilayers can be described in the vicinity of the Dirac frequency by formulating the Hamiltonian from the tight binding model of bilayer graphene. Recently, an acoustic bilayer design was built at a large twist angle of 27.79°, consisting of connected cavities[57]. Strong interlayer coupling was used to generate a bandgap that harbours higher-order topological states.

In the context of elastodynamics, the analogue of TBG for elastic waves was designed by considering two weakly coupled vibrating plates via a thin elastic medium, where each plate is attached with a honeycomb lattice of point masses[15] (Fig. 2e, left). The underlying physics of the interlayer coupling is the interaction of flexural waves hosted by the plates. The authors developed a theoretical model to describe their system based on Germain–Lagrange approximation from the equation of motion governing flexural waves in coupled plates. The twist angle comes into play when describing the mass distribution on both layers. They demonstrated the emergence of flat bands at a magic angle of 1.61° (rightmost panel of Fig. 2e, right). Meanwhile, Martí-Sabaté and Torrent[59] conducted a theoretical study on the interaction of elastodynamic modes with a cluster of scatterers distributed in a moiré pattern over a thin plate. This study disclosed the emergence of dipolar resonances at specific discrete values of the twist angles (Fig. 2f). A plate decorated with a lattice of pillars was constructed with modulated heights in a moiré pattern[61], and topological transition of the isofrequency contour from hyperbolic to elliptical dispersion was demonstrated, similar to what was observed in a previous study in photonics[20]. Very recently, a family of bilayer phononic crystals was presented, where both sides of a plate are decorated with a hexagonal lattice of pillars[60]. A plate with a sufficiently large thickness possesses a weak interlayer coupling between SAWs (surface acoustic waves) propagating on each side of the plate, representing a direct analogue of bilayer graphene. The authors also studied the twisted bilayer phononic crystal under a large commensurate angle of 38.213°, which creates a structure with an even sublattice exchange (SE) symmetry. Furthermore, by reducing the thickness of the plate, strong interlayer coupling can be introduced, which leads to substantial changes in the band structure and the possibility of bilayer valley Hall states under the even SE symmetry.

Outlook

As it currently stands, there are two different research directions for moiré photonic and phononic structures. The first is centred on identifying engineered artificial structures that control waves to emulate the electronic behaviours experimentally observed or theoretically predicted in TBG. The epitome of this effort is the finding of flat bands at magic angles in bilayer photonic[16,19], sonic[14,17] and elastodynamic[15] moiré structures. Whereas it is intriguing to show that the concept of the magic angle can be generalized to virtually all classical wave systems, this twist-induced behaviour (flat bands at the magic angle) has yet to be experimentally observed in a classical wave counterpart of TBG. This is largely because, at small twist angles, the unit cell becomes extremely large, especially for moiré phononic and microwave photonic crystals due to the large wavelength used. Challenges persist even in experiments involving relatively large twist angles. For instance, the observation of topological corner states in even-SE-symmetry TBG is one such challenge[16]. In addition, in acoustic lattices, the thermoviscous loss is a main limiting factor. Furthermore, in contrast to electronic systems, it is relatively easy to engineer flat bands or higher-order topological insulators using monolayer photonic and phononic crystals[63]. Therefore, it is crucial to elucidate the benefit of the twist-induced flat bands or topological corner modes in classical wave systems. Although moiré crystals are tunable in nature due to their twist degree of freedom, and the results produced from classical wave systems can advance research into TBG or twistronics in general by informing the discovery of new quantum materials, future work directions could leverage the engineering of flat bands and higher-order band topology for practical functionalities such as robust dynamic energy trapping via the twist, which could benefit the fields of nonlinear photonics and optomechanics.

The second direction entails a broader scope, and it seeks to expand the field of artificial photonic and phononic crystals by taking inspiration from TBG in that the twist degree of freedom and interlayer coupling, or simply the moiré pattern, are harnessed to give rise to new design paradigms of classical wave devices. This line of research often leads to results that represent an important departure from TBG in that these results find no counterparts in TBG[20,45,60]. Although notable progress has been made in the development of moiré crystals, there remains a need to explore their integration into functional devices that can leverage twist and interlayer coupling for precise wave control. One potential application involves the use of moiré patterns in acoustofluidics to create customizable fluid-streaming patterns for the manipulation and trapping of microparticles. To achieve this goal, further research is needed to investigate the physics of acoustic streaming that is enabled by moiré patterns in fluids for the application of moiré phononic structures in fluid-flow manipulation.

Going forwards, there is a plethora of directions that can be explored to bring the field of moiré photonic and phononic crystals to the next phase. For example, loss and gain can be added into the equation to enrich the physics of moiré photonic and phononic crystals, where the interplay between loss and gain can be further complemented by twist and interlayer coupling. It is noted that two recent papers have theoretically studied parity-time-symmetric AA- and AB-stacked bilayer photonic graphene[64,65], and showed that parity-time symmetry induces band alteration in the vicinity of the Dirac point[65] as well as the existence of exceptional concentric rings with particular topological features[64]. Another direction is to leverage the unique strength of photonic and phononic crystals (or metasurfaces), where arbitrary 2D lattices other than the honeycomb lattice can be readily built, and their interaction with twist and interlayer coupling can be theoretically or even experimentally probed. In this spirit, bilayer square lattice photonic crystals and photonic moiré patterns resulting from square lattices have recently been studied[40,45]. However, other lattices, such as the kagome lattice, have largely been unexplored in classical waves. In addition, while in electronic materials the nearest-interlayer hopping is naturally the strongest, photonic and phononic crystals can be a robust platform to engineer interlayer coupling, where long-range interlayer hopping can be made stronger than nearest-interlayer hopping. Recent studies have demonstrated that long-range hopping stronger than nearest-neighbour hopping can extend the topological order to a new topological class, giving rise to a greater number of topologically protected states in a 2D monolayer crystal[66]. We expect that similar novel large-chiral-number topological states can be uncovered in the moiré system.

Another avenue of research that has recently come to light involves the exploration of bound states in the continuum (BICs) within twisted bilayer phononic and photonic crystals. BICs are localized modes that can be present in the continuous spectrum of propagating or radiating waves but cannot interact with any of these waves. A unique BIC has been observed in the continuum of a bilayer photonic crystal, emerging from the coupling between transverse electric and transverse magnetic modes, arising from a broken symmetry in the bilayer structure[67]. In another study, twisted bilayer photonic crystal slabs were constructed to exhibit a quasi-BIC by manipulating the twist and interlayer coupling[41]. Very recently, a mirror-stacking approach was developed to construct symmetry-protected topological BICs[68] in acoustics. Such realizations provide further insights into the emergence of BICs for efficient localization of light and sound in moiré photonic and phononic structures. On the same front of wave localization, an encouraging avenue worth exploring involves the introduction of

topological defects into moiré photonic and phononic structures. In these scenarios, the twist can alter the interaction among defect states between the layers, giving rise to new defect modes. This, in turn, could suggest potential applications for enhanced and loss-immune communication, lasing and sensing.

Meanwhile, nonlinear optical responses of TBG have been investigated to demonstrate higher-order harmonic responses that are absent in monolayer or conventional bilayer graphene, spawning the field of optotwistronics[69,70]. Nonlinear optical waves have also been studied extensively in photonic crystals, leading to applications towards reduced-size multifunctional control of light, photonic circuits for optical communication and multiphoton absorption. In mechanical waves, nonlinear dynamical behaviours have also been studied in phononic crystals to achieve subwavelength wave control[71], acoustic nonreciprocity[72], soft material lattices for nonlinear wave control[73] and architected lattices for soliton manpulation[74,75]. However, nonlinear dynamic responses of twisted bilayer photonic and phononic crystals have yet to be explored. By incorporating the twist degree of freedom in conjunction with interlayer coupling, photonic and phononic crystals can achieve a whole new level of capability with highly customizable nonlinear dynamic behaviour, which has the potential to revolutionize photonics and acoustics, leading to remarkable technological breakthroughs.

Beyond passive moiré lattices, an exciting avenue of exploration involves designing bilayer lattices with controlled nonreciprocal interactions between the layers, which would involve an active system[76]. The combination of the twist and nonreciprocal interlayer coupling has the potential to expand the capabilities of twister bilayer lattices for wave manipulation. In the same direction for active systems, instead of considering a static twist, it is worth exploring the dispersion of classical waves of a dynamic moiré lattice. This dynamic rotation induces a spacetime modulation of the periodicity and/or quasiperiodicity of the bilayer lattice, hence its effective properties, which could potentially lead to exciting phenomena related to nonreciprocity. A bilayer structure with a rotating moiré pattern could offer a simple and efficient method to achieve spatiotemporal modulation. This approach is expected to be more relevant for acoustic waves due to their lower frequencies, although the flow generated by the rotation could present challenges for the experiment.

Overall, as research in TBG continues to advance and the broader field of twistronics becomes increasingly multidisciplinary, we anticipate sustained growth in the subject of moiré photonic and phononic structures throughout the coming decade. In addition to the aforementioned exploratory directions, with the rapid evolution of fabrication and characterization techniques, in the future we foresee the emergence of novel moiré platforms for classical waves. These platforms may draw inspiration from advancements in twisted electronic heterostructures or involve the creation of innovative moiré structures beyond the equivalent of TBG for efficient wave control.

References

1. Geim, A. K. & Grigorieva, I. V. Van der Waals heterostructures. *Nature* **499**, 419–425 (2013).
2. Carr, S. et al. Twistronics: manipulating the electronic properties of two-dimensional layered structures through their twist angle. *Phys. Rev. B* **95**, 075420 (2017).
3. Rozhkov, A. V., Sboychakov, A. O., Rakhmanov, A. L. & Nori, F. Electronic properties of graphene-based bilayer systems. *Phys. Rep.* **648**, 1–104 (2016).
4. Nam, N. N. T. & Koshino, M. Lattice relaxation and energy band modulation in twisted bilayer graphene. *Phys. Rev. B* **96**, 075311 (2017).
5. Bistritzer, R. & MacDonald, A. H. Moiré bands in twisted double-layer graphene. *Proc. Natl Acad. Sci. USA* **108**, 12233–12237 (2011).
6. Sunku, S. S. et al. Photonic crystals for nano-light in moiré graphene superlattices. *Science* **362**, 1153–1156 (2018).
7. Moon, P. & Koshino, M. Optical absorption in twisted bilayer graphene. *Phys. Rev. B* **87**, 205404 (2013).
8. Li, H. et al. Thermal conductivity of twisted bilayer graphene. *Nanoscale* **6**, 13402–13408 (2014).
9. Cao, Y. et al. Correlated insulator behaviour at half-filling in magic-angle graphene superlattices. *Nature* **556**, 80–84 (2018).
10. Cao, Y. et al. Unconventional superconductivity in magic-angle graphene superlattices. *Nature* **556**, 43–50 (2018).
11. Lu, X. et al. Superconductors, orbital magnets and correlated states in magic-angle bilayer graphene. *Nature* **574**, 653–657 (2019).
12. Yankowitz, M. et al. Tuning superconductivity in twisted bilayer graphene. *Science* **363**, 1059–1064 (2019).
13. Po, H. C., Zou, L., Vishwanath, A. & Senthil, T. Origin of Mott insulating behavior and superconductivity in twisted bilayer graphene. *Phys. Rev. X* **8**, 031089 (2018).
14. Deng, Y. et al. Magic-angle bilayer phononic graphene. *Phys. Rev. B* **102**, 180304(R) (2020).
15. Rosendo López, M., Peñaranda, F., Christensen, J. & San-Jose, P. Flat bands in magic-angle vibrating plates. *Phys. Rev. Lett.* **125**, 214301 (2020).
16. Oudich, M. et al. Photonic analog of bilayer graphene. *Phys. Rev. B* **103**, 214311 (2021).
17. Gardezi, S. M., Pirie, H., Carr, S., Dorrell, W. & Hoffman, J. E. Simulating twistronics in acoustic metamaterials. *2D Mater.* **8**, 031002 (2021).
18. Tang, H. et al. Modeling the optical properties of twisted bilayer photonic crystals. *Light Sci. Appl.* **10**, 157 (2021).
19. Dong, K. et al. Flat bands in magic-angle bilayer photonic crystals at small twists. *Phys. Rev. Lett.* **126**, 223601 (2021).
20. Hu, G. et al. Topological polaritons and photonic magic angles in twisted α-MoO_3 bilayers. *Nature* **582**, 209–213 (2020).
21. Du, L. et al. Moiré photonics and optoelectronics. *Science* **379**, eadg0014 (2023).
22. Correas-Serrano, D., Gomez-Diaz, J. S., Melcon, A. A. & Alù, A. Black phosphorus plasmonics: anisotropic elliptical propagation and nonlocality-induced canalization. *J. Opt.* **18**, 104006 (2016).
23. Dai, Z. et al. Edge-oriented and steerable hyperbolic polaritons in anisotropic van der Waals nanocavities. *Nat. Commun.* **11**, 6086 (2020).
24. Chen, M. et al. Configurable phonon polaritons in twisted α-MoO_3. *Nat. Mater.* **19**, 1307–1311 (2020).
25. Wang, C. et al. Van der Waals thin films of WTe_2 for natural hyperbolic plasmonic surfaces. *Nat. Commun.* **11**, 1158 (2020).
26. Hu, G., Krasnok, A., Mazor, Y., Qiu, C.-W. & Alù, A. Moiré hyperbolic metasurfaces. *Nano Lett.* **20**, 3217–3224 (2020).
27. Gomez-Diaz, J. S. & Alù, A. Flatland optics with hyperbolic metasurfaces. *ACS Photonics* **3**, 2211–2224 (2016).
28. Kotov, O. V. & Lozovik, Yu. E. Hyperbolic hybrid waves and optical topological transitions in few-layer anisotropic metasurfaces. *Phys. Rev. B* **100**, 165424 (2019).
29. Hu, G., Zheng, C., Ni, J., Qiu, C.-W. & Alù, A. Enhanced light–matter interactions at photonic magic-angle topological transitions. *Appl. Phys. Lett.* **118**, 211101 (2021).
30. Zheng, Z. et al. Phonon polaritons in twisted double-layers of hyperbolic van der Waals crystals. *Nano Lett.* **20**, 5301–5308 (2020).
31. Zhang, X., Zhong, Y., Low, T., Chen, H. & Lin, X. Emerging chiral optics from chiral interfaces. *Phys. Rev. B* **103**, 195405 (2021).
32. Stauber, T., Low, T. & Gómez-Santos, G. Chiral response of twisted bilayer graphene. *Phys. Rev. Lett.* **120**, 046801 (2018).
33. Wu, B.-Y., Shi, Z.-X., Wu, F., Wang, M.-J. & Wu, X.-H. Strong chirality in twisted bilayer α-MoO_3. *Chin. Phys. B* **31**, 044101 (2022).

34. Lin, X. et al. Chiral plasmons with twisted atomic bilayers. *Phys. Rev. Lett.* **125**, 077401 (2020).
35. Wang, J., Bo, W., Ding, Y., Wang, X. & Mu, X. Optical, optoelectronic, and photoelectric properties in moiré superlattices of twist bilayer graphene. *Mater. Today Phys.* **14**, 100238 (2020).
36. Mao, X.-R., Shao, Z.-K., Luan, H.-Y., Wang, S.-L. & Ma, R.-M. Magic-angle lasers in nanostructured moiré superlattice. *Nat. Nanotechnol.* **16**, 1099–1105 (2021).
37. Wang, H., Ma, S., Zhang, S. & Lei, D. Intrinsic superflat bands in general twisted bilayer systems. *Light Sci. Appl.* **11**, 159 (2022).
38. Garcia-Vidal, F. J. et al. Spoof surface plasmon photonics. *Rev. Mod. Phys.* **94**, 025004 (2022).
39. Gao, Z. et al. Valley surface-wave photonic crystal and its bulk/edge transport. *Phys. Rev. B* **96**, 201402 (2017).
40. Lou, B. et al. Theory for twisted bilayer photonic crystal slabs. *Phys. Rev. Lett.* **126**, 136101 (2021).
41. Huang, L., Zhang, W. & Zhang, X. Moiré quasibound states in the continuum. *Phys. Rev. Lett.* **128**, 253901 (2022).
42. Lou, B., Wang, B., Rodríguez, J. A., Cappelli, M. & Fan, S. Tunable guided resonance in twisted bilayer photonic crystal. *Sci. Adv.* **8**, eadd4339 (2022).
43. Lou, B. & Fan, S. Tunable frequency filter based on twisted bilayer photonic crystal slabs. *ACS Photon.* **9**, 800–805 (2022).
44. Yi, C.-H., Park, H. C. & Park, M. J. Strong interlayer coupling and stable topological flat bands in twisted bilayer photonic Moiré superlattices. *Light Sci. Appl.* **11**, 289 (2022).
45. Wang, P. et al. Localization and delocalization of light in photonic moiré lattices. *Nature* **577**, 42–46 (2020).
46. Mahmood, R., Ramirez, A. V. & Hillier, A. C. Creating two-dimensional quasicrystal, supercell, and Moiré lattices with laser interference lithography: implications for photonic bandgap materials. *ACS Appl. Nano Mater.* **4**, 8851–8862 (2021).
47. Lubin, S. M., Hryn, A. J., Huntington, M. D., Engel, C. J. & Odom, T. W. Quasiperiodic moiré plasmonic crystals. *ACS Nano* **7**, 11035–11042 (2013).
48. Zhang, Y. et al. Unfolded band structures of photonic quasicrystals and moiré superlattices. *Phys. Rev. B* **105**, 165304 (2022).
49. Guan, J. et al. Far-field coupling between moiré photonic lattices. *Nat. Nanotechnol.* **18**, 514–520 (2023).
50. Wang, W. et al. Moiré fringe induced gauge field in photonics. *Phys. Rev. Lett.* **125**, 203901 (2020).
51. Hong, P. et al. Flatband mode in photonic moiré superlattice for boosting second-harmonic generation with monolayer van der Waals crystals. *Opt. Lett.* **47**, 2326–2329 (2022).
52. Nguyen, H. S. et al. Symmetry breaking in photonic crystals: on-demand dispersion from flatband to Dirac cones. *Phys. Rev. Lett.* **120**, 066102 (2018).
53. Nguyen, D. X. et al. Magic configurations in moiré superlattice of bilayer photonic crystals: almost-perfect flatbands and unconventional localization. *Phys. Rev. Res.* **4**, L032031 (2022).
54. Talukdar, T. H., Hardison, A. L. & Ryckman, J. D. Moiré effects in silicon photonic nanowires. *ACS Photon.* **9**, 1286–1294 (2022).
55. Dorrell, W., Pirie, H., Gardezi, S. M., Drucker, N. C. & Hoffman, J. E. van der Waals metamaterials. *Phys. Rev. B* **101**, 121103 (2020).
56. Lu, J. et al. Valley topological phases in bilayer sonic crystals. *Phys. Rev. Lett.* **120**, 116802 (2018).
57. Wu, S.-Q. et al. Higher-order topological states in acoustic twisted moiré superlattices. *Phys. Rev. Appl.* **17**, 034061 (2022).
58. López, M. R., Zhang, Z., Torrent, D. & Christensen, J. Theory of holey twistsonic media. *Commun. Mater.* **3**, 99 (2022).
59. Martí-Sabaté, M. & Torrent, D. Dipolar localization of waves in twisted phononic crystal plates. *Phys. Rev. Appl.* **15**, L011001 (2021).
60. Oudich, M., Deng, Y. & Jing, Y. Twisted pillared phononic crystal plates. *Appl. Phys. Lett.* **120**, 232202 (2022).
61. Yves, S. et al. Moiré-driven topological transitions and extreme anisotropy in elastic metasurfaces. *Adv. Sci.* **9**, 2200181 (2022).
62. Jin, Y., Wang, W., Wen, Z., Torrent, D. & Djafari-Rouhani, B. Topological states in twisted pillared phononic plates. *Extreme Mech. Lett.* **39**, 100777 (2020).
63. Tang, L. et al. Photonic flat-band lattices and unconventional light localization. *Nanophotonics* **9**, 1161–1176 (2020).
64. Wang, H. et al. Exceptional concentric rings in a non-Hermitian bilayer photonic system. *Phys. Rev. B* **100**, 165134 (2019).
65. Zhang, D. et al. PT-symmetric non-Hermitian AB-stacked bilayer honeycomb photonic lattice. *J. Opt. Soc. Am. B* **37**, 3407–3413 (2020).
66. Wang, D. et al. Realization of a $\mathbb{Z}$-classified chiral-symmetric higher-order topological insulator in a coupling-inverted acoustic crystal. *Phys. Rev. Lett.* **131**, 157201 (2023).
67. Wang, H.-F. et al. Bound states in the continuum in a bilayer photonic crystal with TE–TM cross coupling. *Phys. Rev. B* **98**, 214101 (2018).
68. Liu, L., Li, T., Zhang, Q., Xiao, M. & Qiu, C. Universal mirror-stacking approach for constructing topological bound states in the continuum. *Phys. Rev. Lett.* **130**, 106301 (2023).
69. Di Mauro Villari, L. & Principi, A. Optotwistronics of bilayer graphene. *Phys. Rev. B* **106**, 035401 (2022).
70. Zhang, Y., Qin, Y., Zheng, H. & Ren, H. The evolution of the solitons in periodic photonic moiré lattices controlled by rotation angle with saturable self-focusing nonlinearity media. *Laser Phys.* **32**, 045401 (2022).
71. Fang, X., Wen, J., Bonello, B., Yin, J. & Yu, D. Ultra-low and ultra-broad-band nonlinear acoustic metamaterials. *Nat. Commun.* **8**, 1288 (2017).
72. Librandi, G., Tubaldi, E. & Bertoldi, K. Programming nonreciprocity and reversibility in multistable mechanical metamaterials. *Nat. Commun.* **12**, 3454 (2021).
73. Guo, X., Gusev, V. E., Tournat, V., Deng, B. & Bertoldi, K. Frequency-doubling effect in acoustic reflection by a nonlinear, architected rotating-square metasurface. *Phys. Rev. E* **99**, 052209 (2019).
74. Deng, B., Raney, J. R., Tournat, V. & Bertoldi, K. Elastic vector solitons in soft architected materials. *Phys. Rev. Lett.* **118**, 204102 (2017).
75. Deng, B., Wang, P., He, Q., Tournat, V. & Bertoldi, K. Metamaterials with amplitude gaps for elastic solitons. *Nat. Commun.* **9**, 3410 (2018).
76. Wang, X. et al. A scheme for realizing nonreciprocal interlayer coupling in bilayer topological systems. *Front. Optoelectron.* **16**, 38 (2023).
77. Motycka, J. A grazing-incidence moire interferometer for displacement and planeness measurement. *Exp. Mech.* **15**, 279–281 (1975).
78. Khan, M. T. I., Kazuhiko, M., Teramoto, K. & Hasan, M. M. Precise measurement of moving object by moiré-based image processing technique. *Open J. Fluid Dyn.* **2**, 202–207 (2012).
79. Sharpe, A. L. et al. Emergent ferromagnetism near three-quarters filling in twisted bilayer graphene. *Science* **365**, 605–608 (2019).
80. Ikeda, T. N. High-order nonlinear optical response of a twisted bilayer graphene. *Phys. Rev. Res.* **2**, 032015 (2020).
81. Katz, O., Refael, G. & Lindner, N. H. Optically induced flat bands in twisted bilayer graphene. *Phys. Rev. B* **102**, 155123 (2020).
82. Kort-Kamp, W. J. M., Culchac, F. J., Capaz, R. B. & Pinheiro, F. A. Photonic spin Hall effect in bilayer graphene moiré superlattices. *Phys. Rev. B* **98**, 195431 (2018).
83. Polshyn, H. et al. Large linear-in-temperature resistivity in twisted bilayer graphene. *Nat. Phys.* **15**, 1011–1016 (2019).

84. Alborzi, M. S., Rajabpour, A. & Montazeri, A. Heat transport in 2D van der Waals heterostructures: an analytical modeling approach. *Int. J. Therm. Sci.* **150**, 106237 (2020).
85. Wang, L. et al. Correlated electronic phases in twisted bilayer transition metal dichalcogenides. *Nat. Mater.* **19**, 861–866 (2020).
86. Tran, K. et al. Evidence for moiré excitons in van der Waals heterostructures. *Nature* **567**, 71–75 (2019).
87. Jin, C. et al. Observation of moiré excitons in WSe_2/WS_2 heterostructure superlattices. *Nature* **567**, 76–80 (2019).
88. Wu, F., Lovorn, T., Tutuc, E. & MacDonald, A. H. Hubbard model physics in transition metal dichalcogenide moiré bands. *Phys. Rev. Lett.* **121**, 026402 (2018).
89. Crasto de Lima, F., Miwa, R. H. & Suárez Morell, E. Double flat bands in kagome twisted bilayers. *Phys. Rev. B* **100**, 155421 (2019).
90. Sinha, M. et al. Twisting of 2D kagomé sheets in layered intermetallics. *ACS Cent. Sci.* **7**, 1381–1390 (2021).
91. Can, O. et al. High-temperature topological superconductivity in twisted double-layer copper oxides. *Nat. Phys.* **17**, 519–524 (2021).
92. Alnasser, K., Kamau, S., Hurley, N., Cui, J. & Lin, Y. Photonic band gaps and resonance modes in 2D twisted moiré photonic crystal. *Photonics* **8**, 408 (2021).
93. Zheng, S. et al. Topological network and valley beam splitter in acoustic biaxially strained moiré superlattices. *Phys. Rev. B* **105**, 184104 (2022).
94. Tang, H., Ni, X., Du, F., Srikrishna, V. & Mazur, E. On-chip light trapping in bilayer moiré photonic crystal slabs. *Appl. Phys. Lett.* **121**, 231702 (2022).
95. Raun, A., Tang, H., Ni, X., Mazur, E. & Hu, E. L. GaN magic angle laser in a merged moiré photonic crystal. *ACS Photon.* **10**, 3001–3007 (2023).

Acknowledgements

Y.J. acknowledges the support of the US National Science Foundation (CMMI 2039463). C.Q. acknowledges financial support from the National Research Foundation (grant no. NRF-CRP26-2021-0004) and IRG from A*STAR (grant no. M22K2c0088 with WBS A-8001322-00-00).

Competing interests

The authors declare no competing interests.

Additional information

Correspondence should be addressed to Chengwei Qiu or Yun Jing.

Peer review information *Nature Materials* thanks the anonymous reviewers for their contribution to the peer review of this work.